NJC

Accepted Manuscript

This is an *Accepted Manuscript*, which has been through the Royal Society of Chemistry peer review process and has been accepted for publication.

Accepted Manuscripts are published online shortly after acceptance, before technical editing, formatting and proof reading. Using this free service, authors can make their results available to the community, in citable form, before we publish the edited article. We will replace this *Accepted Manuscript* with the edited and formatted *Advance Article* as soon as it is available.

You can find more information about *Accepted Manuscripts* in the Information for Authors.

Please note that technical editing may introduce minor changes to the text and/or graphics, which may alter content. The journal's standard Terms & Conditions and the Ethical guidelines still apply. In no event shall the Royal Society of Chemistry be held responsible for any errors or omissions in this *Accepted Manuscript* or any consequences arising from the use of any information it contains.

ROYAL SOCIETY OF CHEMISTRY

www.rsc.org/njc

Journal Name

ARTICLE

Syntheses and characterizations of six Co(II) and Mn(II) coordination polymers based on amino-substituted 5-aminoisophthalate and flexible bis(imidazolyl) ligands

Received 00th January 20xx,
Accepted 00th January 20xx

DOI: 10.1039/x0xx00000x

www.rsc.org/

Xiaoju Li,*[a,b] Xiaofei Sun [a,b] Xinxiong Li [b] and Xiahong Xu[a]

Six Co(II) and Mn(II) coordination polymers, $[Co(BIMB)(AIP)]_n$ (**1**), $[Co(BIMB)_{0.5}(H_2O)(AIP)]_n$ (**2**), $[Co(BMIB)_{0.5}(AIP)]_n\cdot(H_2O)_n$ (**3**), $[Mn_2(BIMB)_2(AIP)_2]_n$ (**4**), $[Mn(BMIB)(H_2O)_2(AIP)]_n\cdot(DMF)_n$ (**5**) and $[Mn(BIMB)_{0.5}(PAIP)]_n\cdot(H_2O)_n$ (**6**) (AIP = 5-aminoisophthalate, PAIP = 5-(2-pyridylmethyl)aminoisophthalate, BIMB = 1,4-bis(imidazol-1-yl-methyl)benzene and BMIB = 1,4-bis(2-methylimidazol-1-yl-methyl)benzene), were synthesized and well characterized. AIP in **1**-**5** originates from *in situ* deprotection of 5-(4-oxopentan-2-ylideneamino)isophthalic acid in synthetic process. Complex **1** is a 2D→3D interdigitating network, hydrogen bonds between uncoordinated amino and carboxylate oxygen atoms of the adjacent layers further stabilize the 3-D framework. Different from AIP in **1**, amino of AIP in **2** and **3** participates in coordination, μ_3-bridged AIP connects Co(II) into 1-D double chain and 2-D layer, respectively, subsequent bridge by BIMB and BMIB results in the formation of 2-D layer and 2-D pillared-bilayer network, respectively. Notably, the coordinated water in complex **2** may be reversibly removed with the concomitant color change and the maintenance of original structural framework. Amino of AIP in **4** and **5** is not involved in coordination, AIP and *anti*-conformationed BIMB in **4** link Mn(II) into a 2-D layer consisting of dinuclear Mn(II)-carboxylate units, while AIP and *gauche*-conformationed BMIB in **5** links Mn(II) ions into a 1-D chain. Complex **6** is a 3-D pillared-layer structure. It should be mentioned that the extensive hydrogen bonds are formed in complexes **1**-**6**. Magnetic study of complex **4** shows that there is a dominant antiferromagnetic coupling above 40 K, while a weak ferromagnetic order is caused by spin-canting at lower temperature.

Introduction

The design and synthesis of metal-organic coordination polymers are of great importance in supramolecular chemistry and crystal engineering due to their intriguing structures and potential application as functional materials.[1-4] An effective approach for the synthesis of coordination polymers is the judicial selection of bridging ligands that can bind metal ions in different modes. The multidentate organic ligands containing nitrogen and carboxylate groups have been extensively used, and they play different roles in the assembly of coordination polymers.[5] Generally, carboxylate links metal ions or metal clusters into charge-neutral coordination frameworks, further coordination of nitrogen atoms may satisfy the coordination geometry of metal ions, generating coordination polymers with novel structures and functions. In the context, 5-aminoisophthalate (AIP) is one of promising ligands, its two *V*-shaped carboxylate groups may bridge metal ions in multiply coordination modes similar to that of isophthalate, amino group either may take part in coordination in a nonlinear mode, or may serve as a hydrogen bonding donor to form strong hydrogen bonds.[6] The assembly of AIP with metal ions generates various coordination polymers ranging from discrete oligonuclear species to one- (1-D), two- (2-D) and three-dimensional (3-D) networks, but it is still difficult to exactly predict structures and properties of the target products based on AIP. One of the main reasons is that the assembly process of AIP and metal ions is also influenced by lots of other factors, such as coordination geometry of metal ions, counter anions, temperature, solvents and pH values.[7-9] Furthermore, some unexpected organic reaction may occur in amino group of AIP. It is well known that amino is a reactive group, and is ready to be protected and deprotected in organic reactions.[10] Amino protection and deprotection in the assembly process of organic ligands and metal ions may generate unanticipated coordination polymers, which could not be accessible through direct reactions.[11] Although various coordination polymers from AIP are reported, those based on *in situ* deprotected AIP are seldom investigated.

[a] *Fujian Key Laboratory of Polymer Materials, College of Chemistry and Chemical Engineering, Fujian Normal University, Fuzhou, Fujian, 350007, China. E-mail: xiaojuli@fjnu.edu.cn;*
[b] *State Key Laboratory of Structural Chemistry, Fujian Institute of Research on the Structure of Matter, Chinese Academy of Sciences, Fuzhou, Fujian, 350002, China.*

† Electronic Supplementary Information (ESI) available: [The additional Figures, Crystal data and structure refinement results, selected bond lengths and bond angles, simulate and experimental XRD patterns in complexes **1**-**6**]. See DOI: 10.1039/x0xx00000x

In the construction of coordination polymers, the mixed use of carboxylate ligands and bipyridyl ligands represents an attractive route. Assembly of AIP and bipyridyl ligands with metal ions forms various coordination polymers.[12] In comparison with bipyridyl ligands, bis(imidazolyl) ligands are more readily available and possess stronger coordination ability toward transition metal ions.[13,14] Surprisingly, no coordination polymers from the mixed use of AIP and bis(imidazolyl) ligands have been reported hitherto.

In our previous work, we primarily focused on the syntheses of coordination polymers based on coordination-inert 5-substituted isophthalate ligands and flexible bis(imidazolyl) ligands with alkyl linkers between imidazolyl rings.[15] Among them, 5-positioned substitutents of isophthalate derivatives do not participate in coordination, alternatively, their steric and electric natures may impose important effects on the structures and properties of the target products. As a continuation of our research in coordination polymers based on 5-substituted isophthalates, we are interested in 5-(4-oxopentan-2-ylideneamino)isophthalate (OAIP) and 5-(2-pyridylmethyl)aminoisophthalate (PAIP) (Scheme 1), in which

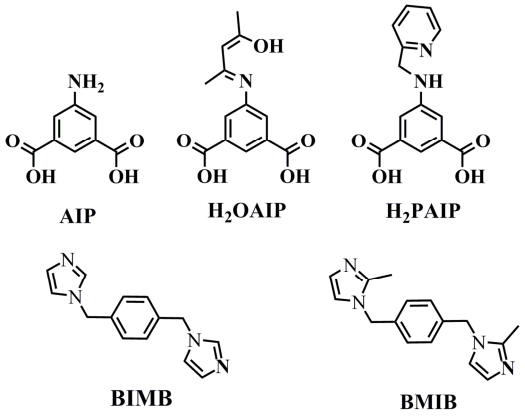

Scheme 1 AIP and the ligands used in this work

five-positioned substitutents of isophthalate are inclined to chelate with metal ions to form a stable chelating ring, resulting in strong competition with imidazolyl nitrogen atoms of flexible bis(imidazolyl) ligands when coordinating to metal centers. Herein, we report the syntheses and characterizations of six coordination polymers, $[Co(BIMB)(AIP)]_n$ (**1**), $[Co(BIMB)_{0.5}(H_2O)(AIP)]_n$ (**2**), $[Co(BMIB)_{0.5}(AIP)]_n\cdot(H_2O)_n$ (**3**), $[Mn_2(BIMB)_2(AIP)_2]_n$ (**4**), $[Mn(BMIB)(H_2O)_2(AIP)]_n\cdot(DMF)_n$ (**5**) and $[Mn(BIMB)_{0.5}(PAIP)]_n\cdot(H_2O)_n$ (**6**) (BIMB = 1,4-bis(imidazol-1-yl-methyl)benzene, BMIB = 1,4-bis(2-methylimidazol-1-yl-methyl)benzene), in which AIP originates from *in situ* deprotection of H_2OAIP or H_2PAIP.

Results and discussion

Synthesis

H_2OAIP is readily available through the condensation reaction of H_2AIP and 2,4-pentanedione. It is known that 5-positioned 4-oxopentan-2-ylideneamino of H_2OAIP either may form a stable six-membered ring with metal ions, or may be deprotected to form AIP under hydrothermal reactions. Sometimes, the deprotection of H_2OAIP in the assembly process may generate new coordination polymers. BIMB and BMIB are known to possess *gauche* and *anti* conformations, which may induce different structural topologies and properties of coordination polymers.[16] Furthermore, the competitive coordination between OAIP and BIMB or BMIB may result in uncoordination of the amino in deprotected OAIP, generating novel supramolecular networks through the directional hydrogen bonds between amino and carboxylate oxygen atoms. In addition, the deprotection of OAIP and subsequent amine coordination to metal ions may be adjusted through changing reaction conditions. The hydrothermal reaction of H_2OAIP, BIMB and $Co(CH_3COO)_2\cdot4H_2O$ gave rise to complex **1**, in which H_2OAIP is deprotected to form AIP, and amino in AIP is not involved in coordination of four-coordinated Co(II), while the use of $Co(NO_3)_2\cdot6H_2O$ under the similar conditions generates complex **2**, in which the deprotected amino takes part in coordination of the octahedral Co(II) ion (Scheme 2). Different from complex **1**,

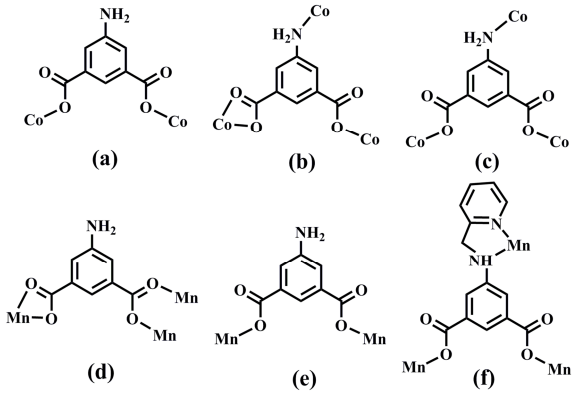

Scheme 2 Coordination modes of AIP and PAIP

hydrothermal reaction of H_2OAIP, BMIB and $Co(CH_3COO)_2\cdot4H_2O$ produces complex **3**, the deprotected amino participates in coordination of four-coordinated Co(II). The variations of Co(II) salts and reaction temperatures have no detectable effect on the structure of **3**. The reaction of H_2OAIP and BIMB/BMIB with $Mn(CH_3COO)_2\cdot4H_2O$ produced **4** and **5**, in which OAIP is deprotected to form AIP. It should be mentioned that we failed to get undeprotected coordination polymers from H_2OAIP, which prompts us to further investigate the assembly of more stable H_2PAIP with metal ions. Recent researches have showed that PAIP may form a stable five-membered chelating ring when coordinating to metal ions,[17] but no coordination polymers based on the mixed ligands of H_2PAIP and nitrogen-donor bridging ligands are reported hitherto. Encouragingly, the reaction of H_2PAIP, BIMB and $Mn(CH_3COO)_2\cdot4H_2O$ produced complex **6**, in which PAIP is undeprotected, and 5-positioned substitutent of PAIP

forms a stable five-membered ring with Mn(II). To our surprise, the reaction of PAIP, BMIB and $Mn(CH_3COO)_2{\cdot}4H_2O$ also afforded complex **5**, in which PAIP is *in situ* deprotected to give rise to AIP.

Structural Descriptions

$[Co(BIMB)(AIP)]_n$ (1). Single crystal X-ray diffraction analysis shows that complex **1** crystallizes in the monoclinic space group $P2_1/c$, and is a 2D→3D interdigitating network. The asymmetric unit consists of one Co(II) ion, one AIP and one BIMB. As shown in Figure 1a, Co1 has a distorted tetrahedral geometry, and is coordinated by two carboxylate oxygen atoms from different AIP and two imidazolyl nitrogen atoms from different BIMB. The average Co-O and Co-N bond distances are 1.993 and 2.009 Å, respectively. AIP adopts a bis-monodentate bridging mode (Scheme 2a), the twisting angles of two carboxylate groups with the central phenyl ring are 2.678(4) and 14.177(4)°, respectively. AIP connects Co(II) into a charge-neutral 1-D $[Co(AIP)]_n$ chain, where the adjacent Co···Co separation is 9.287 Å. BIMB adopts an *anti* conformation, two imidazolyl rings are almost perpendicular to the central phenyl ring, the dihedral angles between imidazolyl rings and phenyl rings are 85.406 and 74.313°, respectively. BIMB further links 1-D chains into a corrugated 2-D layer (Figure 1b), in which Co···Co distance across BIMB is 14.241 Å. The long Co···Co separations across BIMB and AIP generate the large voids in the individual 2-D network, the absence of guest molecules in the voids results in the interdigitation of each 2-D layer with the adjacent independent 2-D layers, finally forming a 2D→3D interdigitating network (Figure S1).[18] It should be mentioned that such 2-D layers in the 3-D framework are packed in an ABAB mode (Figure S2). Amino of AIP is not involved in coordination with Co(II), but it forms hydrogen bonds with coordinated oxygen atoms from the adjacent layer [N1-H1A···O4^{i} 3.056(3) Å, N1-H1B···O1^{ii} 2.956(3) Å, symmetry code: (i) *-x*, *-y*+2, *-z*+2, (ii) *-x*+1, *-y*+2, *-z*+2], which further stabilize the whole structural framework. In order to better understand the interdigitating framework, the topological analysis was carried out. Each window of 2-D network can be regarded as encircling two rods passing through it, giving rise to an increment of overall dimensions from 2-D to 3-D (Figure 1c).

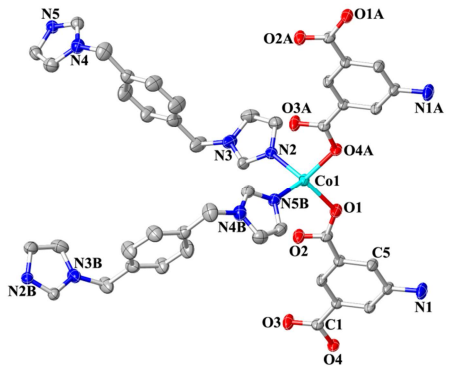

Figure 1a View of coordination environment of Co(II) in **1** with thermal ellipsoids at 50% probability.

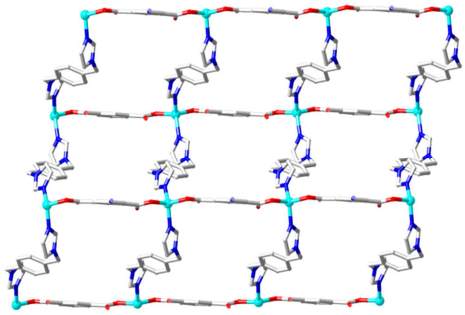

Figure 1b View of 2-D $[Co(BIMB)(AIP)]_n$ layer in **1**.

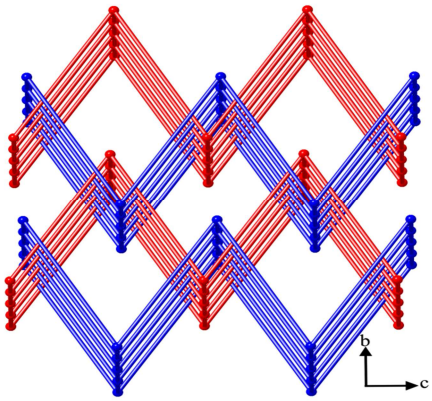

Figure 1c Topological view of 2D→3D network along the *a* axis in **1**.

$[Co(BIMB)_{0.5}(H_2O)(AIP)]_n$ (2). Complex **2** crystallizes in the triclinic space group *P*-1. As shown in Figure 2a, Co(II) ion is in a distorted octahedral geometry, and is coordinated by one monodentate carboxylate oxygen atom, two chelating carboxylate oxygen atoms and one amino from three different AIP, one imidazolyl nitrogen atom and one water molecule complete six-coordinated environment of Co1. The equatorial plane is defined by three oxygen atoms from AIP [O1, O2 and O4A] and water (O1W), the mean deviation of Co1 from the equatorial plane is 0.0827 Å. The amino nitrogen atom (N3B) and imidazolyl nitrogen atom (N1) occupy the axial positions with the N1-Co1-N3B bond angle being 172.57(7)°. The Co1-N1 bond distance of 2.087(2) Å is shorter than the Co1-N3B bond distance of 2.198(2) Å, which suggests that imidazolyl possesses stronger coordination ability than amino group. Each AIP bridges three Co(II) ions through amino group, monodentate and chelating carboxylate groups (Scheme 2b), resulting in the formation of a charge-neutral $[Co(AIP)]_n$ double chain, in which two symmetry-related Co(II) and two AIP form a 14-membered macrocycle with Co···Co separation being 8.088 Å (Figure 2b). Monodentate and chelating carboxylate groups in AIP are highly distorted with respect to the central phenyl ring, the twisting angle between carboxylate and phenyl ring are 27.179(2) and 24.255(2)°, respectively. BIMB adopts an *anti* conformation, two imidazolyl rings are parallel with each other owing to center symmetry, and they are almost perpendicular to the central phenyl ring with the

dihedral angle between imidazolyl and phenyl ring being 84.091(2)°. BIMB bridges the adjacent double chains to generate a 2-D layer (Figure 2b), in which two BIMB, two AIP and two Co(II) ions form a macrocycle. Co···Co separation across BIMB in the macrocycle is 12.555 Å, which is longer than that in complex **1**. Interestingly, water molecule forms a strong intralayer hydrogen bond with the adjacent uncoordinated oxygen atom of monodentate carboxylate [O1W-H1W1···O3^{i} 2.713(3) Å, symmetry code: (i) *x*, *y*+1, *z*], hydrogen bonds among water, amino and carboxylate oxygen atoms [O1W-H1W2···O1^{ii} 2.844(3) Å, N3-H3A···O2^{iii} 3.028(3) Å, symmetry code: (ii) *x*-1, *y*, *z*, (iii) *x*+1, *y*, *z*] extend 2-D layers into a 3-D supramolecular network (Figure 2c).

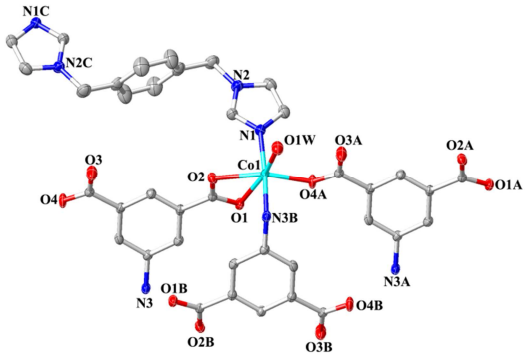

Figure 2a View of coordination environment of Co(II) in **2** with thermal ellipsoids at 50% probability.

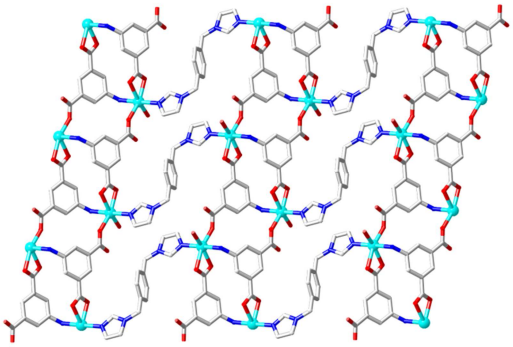

Figure 2b View of 2-D layer in 2.

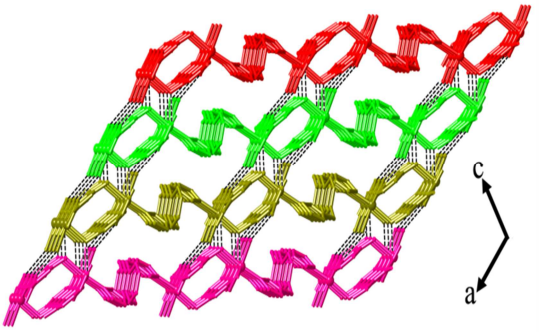

Figure 2c View of 3-D suparmolecular network along the *b* axis in **2.**

$[Co(BMIB)_{0.5}(AIP)]_n \cdot (H_2O)_n$ (3). Complex **3** crystallizes in the monoclinic space group $P2_1/c$, and is a 2-D pillared-bilayer structure. The asymmetric unit consists of one Co(II) ion, one AIP, half of BMIB and one lattice water molecule. As shown in Figure 3a, Co1 is in a distorted tetrahedral geometry, and is coordinated by one 2-methylimidazolyl nitrogen atom from BMIB, two carboxylate oxygen atoms and one amino nitrogen atom from three different AIP. The Co-O/N bond distances are in the range of 1.9566(12)-2.0922(14) Å, which are comparable with those in **1** and **2**. AIP bridges three Co(II) ions through two monodentate carboxylate groups and amino nitrogen atom (Scheme 2c). Two carboxylate groups are almost coplanar with the central phenyl ring with the dihedral angle between carboxylate and phenyl ring being 7.580(2) and 2.481(1)°, respectively. Different from complex **2**, AIP connect Co(II) ions into a 2-D $[Co_3(AIP)_3]_n$ layer (Figure 3b). The layer contains 21-membered macrocycles consisting of three Co(II) and three AIP. The adjacent Co···Co separations in the macrocycle are 7.875, 8.789 and 8.950 Å, respectively. Notably, a pair of such 2-D layers is pillared by BMIB to form a pillared-bilayer network.[22] The bilayer network contains 1-D channels, which are occupied by guest water molecules through hydrogen bonds between water and uncoordinated carboxylate oxygen atom [O1W-H1W1···O2 2.963(3) Å]. BMIB adopts an *anti* conformation, two 2-methylimidazolyl rings are parallel with each other owing to center symmetry, the dihedral angle between 2-methylimidazolyl ring and the central phenyl ring is 85.835(7)°. The Co···Co distance across BMIB is 13.611 Å. Interestingly, the neighboring bilayers are connected with each other by hydrogen bonds between amino and carboxylate oxygen atoms [N1-H1A···O1^{i} 3.0291(18) Å, N1-H1B···O3^{ii} 3.0920(18) Å, symmetry code: (i) -*x*+1, *y*-1/2, -*z*+5/2. (ii) -*x*+1, -*y*-1, -*z*+2], resulting in the formation of a 3-D supramolecular network (Figure 3c).

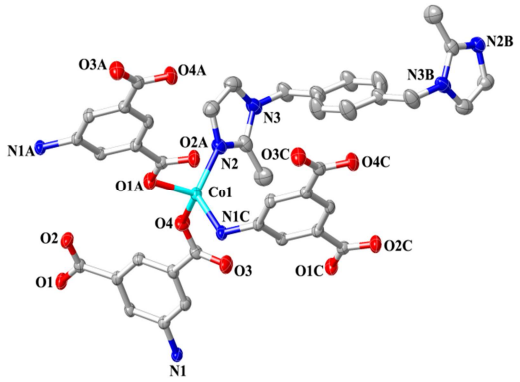

Figure 3a View of coordination environment of Co(II) in **3** with thermal ellipsoids at 50% probability.

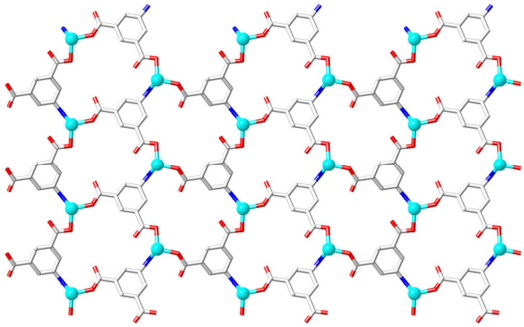

Figure 3b View of 2-D $[Co_3(AIP)_3]_n$ layer in **3**.

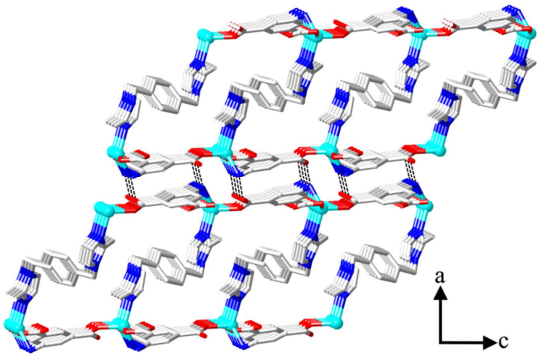

Figure 3c View of 3-D supramocular structure formed by pillared-bilayer network along the *b* axis in **3**.

$[Mn_2(BIMB)_2(AIP)_2]_n$ (4). Complex **4** crystallizes in the triclinic space group *P*-1, and is a 2-D layer consisting of dinuclear Mn(II)-carboxylate units. The asymmetric unit is composed of two crystallographically independent Mn(II) ion, two AIP and two bimb. As shown in Figure 4a, both Mn1 and Mn2 are in a distorted octahedral geometry, and are coordinated by two imidazolyl nitrogen atoms from different BIMB at the axial positions. The N7-Mn1-N3 and N10C-Mn2-N6A bond angles are 176.223(58) and 176.345(57)°, respectively. Two oxygen atoms from one chelating carboxylate group and two oxygen atoms from different μ_2,η^2-carboxylate group comprise the equatorial plane. Mn1 and Mn2 are bridged by two μ_2,η^2-carboxylate groups from different AIP to form a dinuclear Mn(II)-carboxylate unit. The Mn1···Mn2 distance in the dinuclear unit is 4.483 Å. In AIP, amino is not involved in coordination, μ_2,η^2-carboxylate and chelating carboxylate groups bridge three Mn(II) ions (Scheme 2d), generating a charge-neutral $[Mn_2(AIP)_2]_n$ chain, in which two Mn(II) and two AIP form a 14-membered macrocycle. Such 1-D chains are connected by BIMB into a 2-D layer (Figure 4b). The Mn···Mn separations across BIMB are 14.143 and 14.261 Å, respectively. Amino locates two sides of 2-D layer and forms hydrogen bonds with carboxylate oxygen atoms from the adjacent layers [N1-H1B···O4^{i} 3.284 Å, symmetry code: (i) -*x*+3, -*y*+1, -*z*+1], resulting in the formation of a 3-D supramolecular network (Figure 4c).

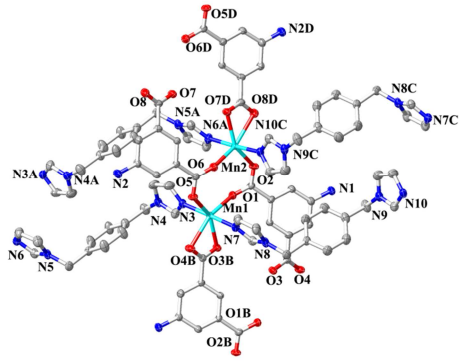

Figure 4a View of coordination environments of Mn(II) in **4** with thermal ellipsoids at 50% probability.

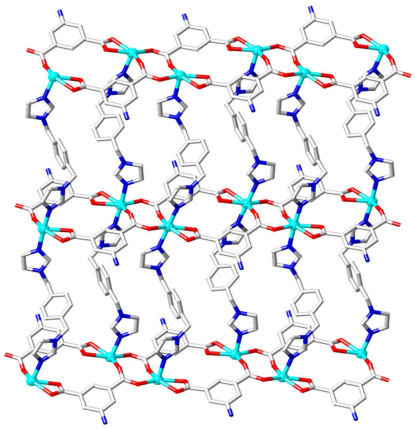

Figure 4b View of 2-D layer in **4.**

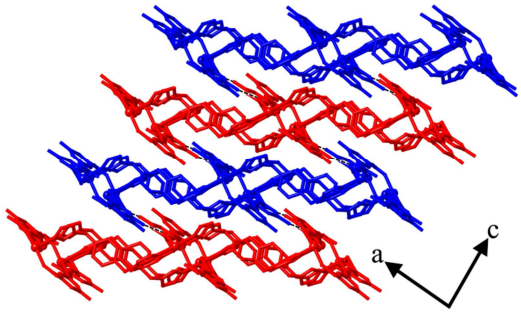

Figure 4c View of 3-D supramolecular network along the *b* axis in **4**.

$[Mn(BMIB)(H_2O)_2(AIP)]_n \cdot (DMF)_n$ (5). Complex **5** crystallizes in the monoclinic space group $P2_1/c$, and is a 1-D chain consisting of 21-membered dinuclear macrocycles. The asymmetric unit contains two crystallographically independent half of Mn(II), one AIP, one BMIB, two coordinated water and one lattice DMF. A shown in Figure 5a, both Mn1 and Mn2 are in a distorted octahedral geometry, and are equivalently coordinated by two carboxylate oxygen atoms from different AIP, two 2-methylimidazolyl nitrogen atoms from differnt BMIB and two water molecules. The Mn-N/O bond distances fall in the range of 2.150(2)-2.284(3) Å. Amino in AIP does not participate in coordination, two carboxylate groups bridge two Mn(II) ions in a bis-monodentate mode (Scheme 2e).

Interestingly, BMIB shows a *gauche* configuration, which is much different from that in complex **3**. Two 2-methylimidazolyl rings in BMIB are almost perpendicular to the central benzyl ring, the twisting angles between 2-methylimidazolyl rings and phenyl ring are 82.839(13) and 84.806(12)°, respectively. AIP and BMIB link Mn(II) ions into a 1-D chain, in which two AIP, two BMIB bridge two Mn(II) ions forming a 21-membered macrocycle. The Mn···Mn distance in the macrocycle is 9.934 Å. In the chain, The coordinated water molecules and uncoordinated carboxylate oxygen atoms form strong intra-chain hydrogen bonds [O1W-H2W···O2 2.74(3) Å, O2W-H3W···O4 2.658(3) Å], while hydrogen bonds between amino and uncoordinated carboxylate oxygen atom [N5-H5B···O4^{i} 3.000(4) Å, symmetry code: (i) *x*, -*y*+3/2, *z*-1/2] as well as between coordinated water and uncoordinated carboxylate oxygen atom [O2W-H4W···O2^{ii} 2.820(3) Å, symmetry code: (ii) *x*, -*y*+3/2, *z*+1/2] extend 1-D chains a 3-D supramolecular network (Figure 5b). Notably, such 3-D network contains 1-D channels. DMF molecules fill the voids of the channels through hydrogen bonds between water and DMF [O1W-H1W···O5^{iii} 2.841(4) Å, symmetry code: (iii) -*x*+1, -*y*+2, -*z*+1], which further stabilizes the whole framework. The accessible void volume is 20.6 % of per unit cell volume after the removal of DMF molecules as calculated by PLATON.

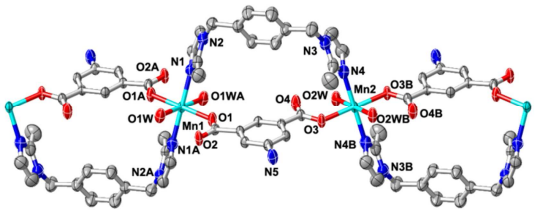

Figure 5a View of coordination environment of Mn(II) in **5** with thermal ellipsoids at 50% probability.

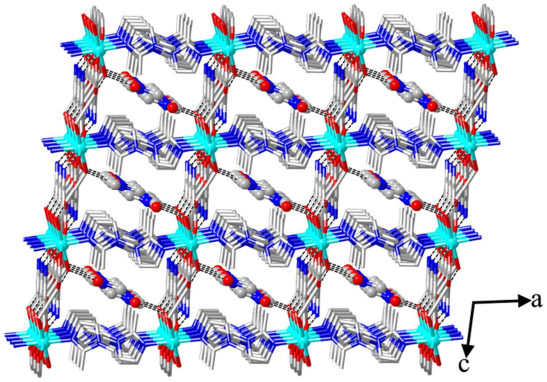

Figure 5b View of 3-D supramolecular network constructed by 1-D chains along the *b* axis in **5**.

[Mn(BIMB)$_{0.5}$(PAIP)]$_n$ (6). Complex **6** crystallizes in the monoclinic space group $P2_1/c$, and is a 3-D pillared-layer network. As shown in Figure 6a, Mn1 is in a distorted MnN_3O_3 octahedral geometry, and is coordinated by one imidazolyl nitrogen atom from BIMB, two chelating nitrogen atoms, two chelating carboxylate oxygen atoms and one monodentate carboxylate oxygen atom from three PAIP. The equatorial plane is defined by three carboxylate oxygen atoms (O1A, O2A and O4B) and amino nitrogen atom (N4), the mean deviation of Mn1 from the equatorial plane is 0.1342 Å. Pyridyl nitrogen atom (N3) and imidazolyl nitrogen atom (N2) occupy the axial positions with the N2-Mn1-N3 bond angle being 172.45(6)°. PAIP bridges three Mn(II) ions through monodentate carboxylate, chelating carboxylate and two chelating nitrogen atoms (Scheme 2f). Pyridyl ring is almost perpendicular to the central phenyl ring with the dihedral angle between them being 86.641°. As shown in Figure 6b, PAIP connects Mn(II) ions into a corrugated [Mn$_3$(PAIP)$_3$]$_n$ layer, in which three Mn(II) and three PAIP form a 63-membered macrocycle with the Mn···Mn distances being 7.779-10.464 Å. BIMB serves as a pillar between adjacent layers, and extends 2-D layers into a 3-D coordination network. The Mn···Mn separation across BIMB is 15.570 Å. Two imidazolyl rings in BIMB are parallel with each other owing to center symmetry, the dihedral angle between imidazolyl ring and phenyl ring is 79.390°. The hydrogen bonds between amino and uncoordinated monodentate carboxylate oxygen atom [N4-H4···O3^{i} 2.966(2) Å, symmetry code: (i) -*x*+1, *y*+1/2, -*z*+1/2] further stabilize the whole framework.

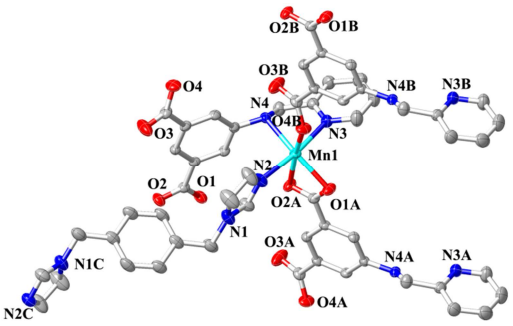

Figure 6a View of coordination environment of Mn(II) in **6** with thermal ellipsoids at 50% probability.

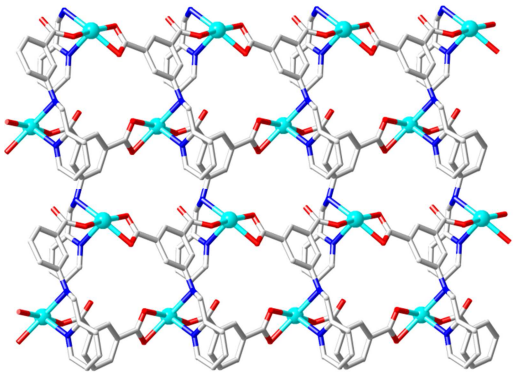

Figure 6b View of 2-D corrugated [Mn(paip)]$_n$ layer in **6.**

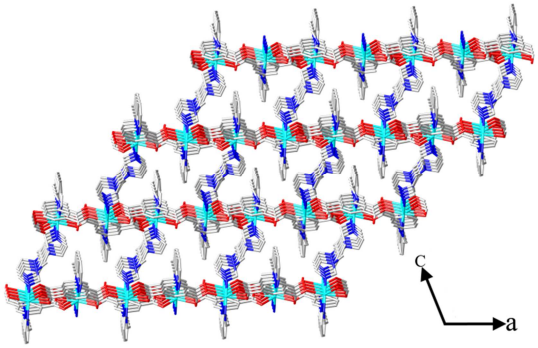

Figure 6c View of 3-D pillared-layer network along the *b* axis in **6**.

Thermogravimetric analysis

Thermal stabilities of complexes **1-6** were investigated using as-synthesized samples under nitrogen atmosphere. Their thermogravimetric analysis (TGA) curves are shown in Figure 7,

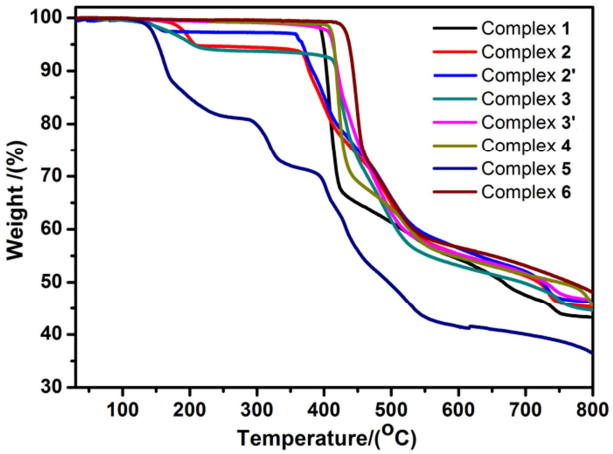

Figure 7 TGA curves of complexes **1**-**6**, dehydrated complex **2** (complex **2'**) and dehydrated complex **3** (complex **3'**).

there is no obvious weight loss before 370 °C in complex **1**. For complex **2**, there is a weight loss of 5.12 % from 150 to 210 °C, corresponding to the release of coordinated water molecules (calcd. 4.80 %), the framework starts to collapse after 350 °C. A weight loss of 4.28% (calcd. 4.62%) was observed from 30 to 215 °C in **3**, which is attributed to the removal of lattice water molecules. The structural frameworks of 3, **4** and **6** are stable up to 400, 405 and 415 °C, respectively. In **5**, the coordinated water and lattice DMF molecules are released from 110 to 240 °C, the weight loss of 18.21 % is close to the theoretical value of 17.90 %, subsequent decomposition of host framework was observed.

Powder X-ray diffraction

In order to check the purity of complexes **1-6**, the as-synthesized samples were measured by powder X-Ray diffraction (XRD) at room temperature. As shown in Figure S3 in supporting information, the peak positions of the experimental patterns are in good agreement with the simulated ones, which clearly demonstrates good purity of these complexes. Notably, when the as-synthesized samples of **2** and **3** were heated to 240°C in order to remove coordinated and lattice water molecules, and then were put into water for one week. XRD studies show that their structural frameworks have no obvious change.

Magnetic properties

Complex **4** consists of dinuclear Mn(II)-carboxylate units, the Mn(II)···Mn(II) distance in the dinuclear unit is 4.483 Å, which suggests there is magnetic exchange within dinulear Mn(II) ions. However, for other Mn(II) and Co(II) coordination polymers, single metal ions are well separated by AIP and bis(imidazolyl) ligands, magnetic exchange between metal ions can be neglected, their magnetic behavior is similar to mononuclear metal ions. As a result, the temperature-dependent magnetic susceptibilities of only complex **4** were measured under a 1000 Oe external field at 2-300 K. The plots of $\chi_m T$ and χ_m^{-1} versus T are shown in Figure 8. $\chi_m T$ value at 300

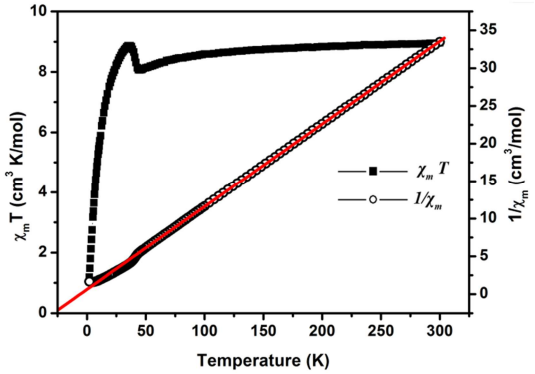

Figure 8 Temperature dependence of the magnetic susceptibility in complex **4**.

K is 8.96 cm^3 K mol^{-1}, which is agreement with the expected value for two non-interacting Mn(II) ions with g = 2.0 and S = 5/2. As temperature decreases, $\chi_m T$ value decreases slightly due to Boltzmann depopulation of the excited states and population of the ground state, suggesting predominant antiferromagnetic coupling. It should be mentioned that $\chi_m T$ value quickly increases below 50 K and reaches the maximum value of 8.87 cm^3 K mol^{-1} at 37 K, and then sharply drops to 1.19 cm^3 K mol^{-1} at 2 K, which indicates the occurrence of onset of a weakly ferromagnetic state caused by spin-canting.[20] The reciprocal value of magnetic susceptibility follows Curie-Weiss law above 50 K with Curie constant C = 5.94 cm^3 K mol^{-1} and Weiss constant θ = –15.77 K. Negative Weiss constant value further indicates predominately antiferromagnetic coupling above this temperature.

Discussion

It is known that 2-methylimidozolyl ring in BMIB possesses the bulkier steric hindrance than imidazolyl ring in BIMB, the bulky hindrance between coordination groups either reduces coordination number of metal ions or results in coordination of small guest molecules. Co(II) ions in **1** and **3** adopt a distorted CoN_2O_2 tetrahedral geometry, but Co(II) in **1** is coordinated by two nitrogen atoms from imdazoly rings of different BIMB, while Co(II) in **3** is coordinated by two nitrogen atoms from 2-methylimidazoyl and AIP, respectively, which is probably ascribed to smaller steric hindrance of amino in AIP. Co(II) in **2** and Mn(II) in **5** are six-coordinated. One water molecule and amino of AIP take part in coordinating in **2**, while the coordination of two small water molecules occurs in **5**. It should be mentioned that the structural framework of **2** is well maintained after the removal of coordinated water, the visual color of crystals was changed from claret to purple (Figure 9),

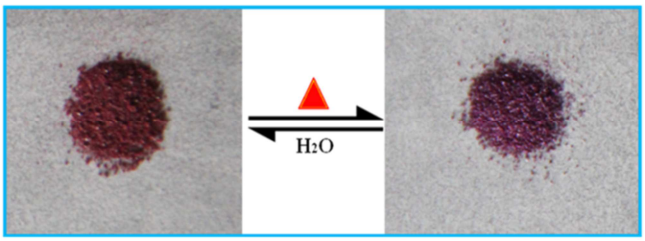

Figure 9 The reversible color change of complex **2** after dehydration and rehydration.

which is attributed to the change of coordination geometry of Co(II) from the distorted octahedron to the distorted trigonal bipyramid after dehydration, resulting in variation of crystal field splitting of Co(II) ions.[21] After the coordinated water molecules were removed, the resultant sample readily absorbs water molecules. In TGA curve of dehydrated complex **2** (complex **2′**), there is a weight loss of 2.42% from 120 to 160 °C, corresponding to half of coordinated water molecules, moreover, the temperature of the weight loss is lower than that in complex 2. The decomposition temperatures of the structural framework in complexes 2 and **2′** are identical with each other (Figure 7). Interestingly, when complex **2′** was put into water for one week, complex **2** can be re-formed. The whole process is reversible as confirmed by XRD patterns (Figure S3). Notably, there is no obvious color change in complex **3** after the removal of lattice water molecules. In TGA curve of complex 3′, no weight loss is observed before its structural framework starts to collapse at 400 °C. Both XRD pattern and TGA curve show that the structural framework of complex **3** is stable after the removal of lattice water molecules. However, complex **5** decomposes after the removal of coordinated water molecules.

Conclusions

Six Co(II) and Mn(II) coordination polymers were synthesized using amino-substituted 5-aminoisophthalates and flexible bis(imidazolyl) ligands. The five-positioned substitutent of OAIP does not form a six-membered chelating ring with metal ions, alternatively, it is deprotected to *in situ* form AIP. Amino of AIP in **1**, **3**, **4** and **5** does not participates in coordination, but AIP connects Co(II) and Mn(II) into different structures. The coordinated amino and two carboxylate groups of AIP in **2** and **3** connect three Co(II) ions into 1-D double chain and 2-D layer, respectively. The structural frameworks of **2** and **3** may be maintained after the removal of coordinated water and guest molecules. In addition, the visual color change is accompanied in **2**. The five-positioned substitutent of PAIP in **6** forms a stable five-membered chelating ring with Mn(II), while the replacement of BIMB by BMIB under the same conditions generates complex **5**, in which PAIP is *in situ* deprotected just as OAIP. It should be mentioned that BMIB in complex **5** shows a *gauche* conformation, while BIMB and BMIB in other complexes adopt an *anti* conformation, the steric hindrance of BIMB and BMIB shows obvious effects on the structures of final products. To our knowledge, this is the first report of the coordination polymers based on AIP and bis(imidazolyl) ligands. In summary, this research has demonstrated that 5-positioned chelating substitutes in AIP derivatives may be *in situ* deprotected to form interesting coordination polymers, which provides an new approach for the assembly of coordination polymers with new structures and functions.

Acknowledgements

This work was supported by Provincial Education Department of Fujian (JA12070), State Key Laboratory of Structural Chemistry (20150015) and Program for Innovative Research Team in Science and Technology in Fujian Province University (IRTSTFJ).

Experimental Section

Materials and General methods

H_2PAIP,[22] BIMB[23] and BMIB[23] were synthesized according to the literature methods. Other chemicals were obtained from commercial sources and were used without further purification. IR spectra (KBr pellets) were recorded on a Magna 750 FT-IR spectrophotometer in the range of 400-4000 cm^{-1}. Powder X-ray diffraction data were recorded on a Philips X'Pert-MPD diffractometer with CuK_α radiation (λ = 1.54056 Å). Thermal stability studies were carried out on a NETSCHZ STA 449C thermoanalyzer under N_2 at a heating rate of 10 °C/min from room temperature to 800 °C. The magnetic susceptibility data were collected on a Quantum Design MPMS model 6000 magnetometer in the temperature range of 2-300 K. C, H and N elemental analyses were determined on an EA1110 CHNS-0 CE element analyzer.

Synthesis of H_2OAIP: A mixture of H_2AIP (1.81 g 10 mmol), 2,4-pentanedione (5.00 g, 50 mmol) and triethyamine (5 mL) in ethanol (50 mL) was stirred for 12 h, the resultant solution was concentrated under the reduced pressure. Water (50 mL) was added into the residue to produce white precipitate. After

filtration and washing with ethanol, the pale-yellow product was obtained. Yield: 0.82g [31% based on H_2AIP]. Anal. Calcd. for $C_{13}H_{13}N_5O_5$ (263.25): C, 59.31; H, 4.98; N, 5.32. Found: C, 59.10; H, 4.68; N, 5.26. ^{1}H NMR (DMSO-d_6) δ: 12.58 (s, 1H), 8.24 (s, 1H), 7.86 (s, 2H), 5.67 (s, 1H), 2.08 (s, 3H), 2.03 (s, 3H). ^{13}C NMR (100 MHZ, DMSO) δ: 196.37, 166.57, 159.28, 139.71, 132.94, 128.04, 126.32, 99.28, 29.41, 19.98. IR (KBr, cm^{-1}): 3516(w), 3134(w), 2925(vw), 1674(vs), 1617(vs), 1589(vs), 1569(vs), 1527(vs), 1426(vs), 1360(vs), 1274(m), 1240(s), 1105(s), 1023(w), 981(vw), 951(m), 901(w),826(w), 781(vs), 740(s), 701(w),651(s), 597(w), 538(m).

Synthesis of [Co(BIMB)(AIP)]$_n$ (1): A mixture of H_2OAIP (43 mg, 0.16 mmol), BIMB (60 mg, 0.25 mmol), $Co(CH_3COO)_2{\cdot}4H_2O$ (63 mg, 0.25 mmol) and H_2O (10 mL) was placed in a Teflon-lined stainless steel vessel (30 mL), and was then heated to 120 °C for 3 days. After cooled to room temperature at a rate of 3 °C·h^{-1}, the purple crystals of 1 were obtained. Yield: 40 mg (53% based on H_2OAIP). Anal. Calcd. for $C_{22}H_{19}N_5O_4Co$ (476.35): C, 55.47; H, 4.02; N, 14.70. Found: C, 55.53; H, 3.94; N, 14.84. IR (KBr, cm^{-1}): 3407(vw), 3357(w), 3257(vw), 3113(w), 3037(vw), 2925(vw), 1622(m), 1581(vs), 1443(w), 1343(s), 1307(vs), 1245(m), 1112(m), 1032(vw), 955(vw), 878(m), 775(m), 730(m), 660(m), 609(vw), 474(w).

Synthesis of [Co(BIMB)$_{0.5}$(H$_2$O)(AIP)]$_n$ (2): A mixture of H_2OAIP (43 mg, 0.16 mmol), BIMB (60 mg, 0.25 mmol), $Co(NO_3)_2{\cdot}6H_2O$ (73 mg, 0.25 mmol), ethanol (1 mL) and deionized water (12 mL) was placed in a Teflon-lined stainless steel vessel (30 mL), and was then heated to 120 °C for 3 days. After cooled to room temperature at a rate of 3 °C·h^{-1}, the red crystals of 2 were obtained. Yield: 30 mg (49% based on H_2OAIP). Anal. Calcd. for $C_{15}H_{14}N_3O_5Co$ (375.22): C, 48.01; H, 3.76; N, 11.20. Found: C, 47.97; H, 3.88; N, 11.26. IR (KBr, cm^{-1}): 3782(vw), 3387(w), 3269(w), 3161(w), 3126(w), 2971(vw), 2366(vw), 1616(s), 1546(vs), 1483(m), 1429(s), 1376(vs), 1232(vw), 1083(m), 995(vw), 968(vw), 945(vw), 832(vw), 783(m), 711(m), 616(vw).

Synthesis of [Co(BMIB)$_{0.5}$(AIP)]$_n$·(H$_2$O)$_n$ (3): A mixture of H_2OAIP (66 mg, 0.25 mmol), BMIB (67 mg, 0.25 mmol), $Co(CH_3COO)_2{\cdot}4H_2O$ (126 mg, 0.50 mmol), NaOH (0.4 mL, 1 mol·L^{-1}) and deionized water (12 mL) was placed in a Teflon-lined stainless steel vessel (30 mL), and was then heated to 120 °C for 3 days. After cooled to room temperature at a rate of 3 °C·h^{-1}, the purple crystals were obtained. Yield: 65 mg (67% based on H_2OAIP). Anal. Calcd. for $C_{16}H_{16}N_3O_5Co$ (389.25): C, 49.37; H, 4.14; N, 10.80. Found: C, 49.11; H, 4.27; N, 11.02. IR (KBr, cm^{-1}): 3549(vw), 3493(vw), 3276(w), 3143(w), 1618(w), 1573(vs), 1548(vs), 1478(w), 1444(s), 1352(vs), 1287(vw), 1186(vw), 1136(m), 1096(s), 1003(w), 965(m), 930(vw), 898(vw), 780(s), 726(s), 679(m), 604(vw), 568(vw), 528(m).

Synthesis of [Mn$_2$(BIMB)$_2$(AIP)$_2$]$_n$ (4): A mixture of H_2OAIP (27 mg, 0.10 mmol), BIMB (48 mg, 0.20 mmol), $Mn(CH_3COO)_2{\cdot}4H_2O$ (74 mg, 0.30 mmol), methanol (5 mL) and deionized water (10 mL) was placed in a Teflon-lined stainless steel vessel (30 mL), and was then heated to 130 °C for 3 days. After cooled to room temperature at a rate of 3 °C·h^{-1}, the yellow crystals were obtained. Yield: 20 mg (21% based on H_2OAIP). Anal. Calcd. for $C_{44}H_{38}N_{10}O_8Mn_2$ (944.72): C, 55.93; H, 4.05; N, 14.82. Found: C, 55.85; H, 4.06; N, 14.83. IR (KBr, cm^{-1}): 3746(vw), 3461(w), 3276(w), 3373(w), 3217(vw), 3093(w), 1611(s), 1538(s), 1465(m), 1433(m), 1382(vs), 1286(w), 1106(w), 1084(m), 1027(w), 998(vw), 932(s), 877(w), 820(vw), 793(s), 760(vw), 679(m), 604(vw), 568(vw), 528(m).

Synthesis of [Mn(BMIB)(H$_2$O)$_2$(AIP)]$_n$·(DMF)$_n$ (5): A mixture of H_2OAIP (27 mg, 0.10 mmol), BMIB (24 mg, 0.10 mmol), $Mn(CH_3COO)_2{\cdot}4H_2O$ (74 mg, 0.30 mmol), DMF (5 mL) and deionized water (5 mL) was placed in a bottle of glass (20 mL), and was then heated to 100 °C for 3 days. After cooled to room temperature, the yellow block crystals were obtained. Yield: 32mg (52% based on H_2OAIP). Anal. Calcd. for $C_{27}H_{34}N_6O_7Mn$ (609.54): C, 53.20; H, 5.62; N, 13.78. Found: C, 52.87; H, 5.69; N, 13.71. IR (KBr, cm^{-1}): 3427(w), 3319(m), 3125(vw), 2953(vw), 2928(vw), 1650(vs), 1593(vs), 1545(vs), 1471(w), 1412(vs), 1362(vs), 1326(w), 1289(m), 1097(w), 1039(vw), 1017(vw), 1000(w), 972(vw), 935(vw), 891(w), 867(w), 784(m), 764(w), 724(w), 710(m), 678(w), 557(vw), 508(vw), 482(vw), 442(vw), 430(vw).

The complex **5** was also prepared when H_2OAIP was replaced by H_2PAIP.

Synthesis of [Mn(BIMB)$_{0.5}$(PAIP)]$_n$·(H$_2$O)$_n$ (6): A mixture of H_2PAIP (54 mg, 0.20 mmol), BIMB (48 mg, 0.20 mmol), $Mn(CH_3COO)_2{\cdot}4H_2O$ (100 mg, 0.40 mmol), ethanol (0.4 mL) and deionized water (12 mL) was placed in a Teflon-lined stainless steel vessel (30 mL), and was then heated to 130 °C for 3 days. After cooled to room temperature at a rate of 3 °C·h^{-1}, brown crystals were obtained. Yield: 27mg (30% based on H_2PAIP). Anal. Calcd. for $C_{21}H_{17}N_4O_4Mn$ (444.33): C, 56.76; H, 3.85; N, 12.60. Found: C, 56.51; H, 4.15; N, 12.64. IR (KBr, cm^{-1}): 3186(vw), 3122(vw), 2901(vw), 2361(vw) 1622(w), 1579(s), 1542(s), 1430(m), 1368(vs), 1237(w), 1215(vw), 1104(w), 1081(w), 1028(vw), 936(vw), 838(vw), 775(m), 738(m), 719(m), 656(vw), 618(vw), 460(vw).

X-Ray Crystallography

Single crystals of complexes **1**-**6** were mounted on a glass fiber for X-ray diffraction analysis. Data sets were collected on a Rigaku AFC7R equipped with a graphite-monochromated Mo-Kα radiation (λ = 0.71073 Å) from a rotating anode generator at 293 K. Intensities were corrected for LP factors and empirical absorption using the ψ scan technique. The structures were solved by direct methods and refined on F^2 with full-matrix least-squares techniques using the SHELX-97 program package.[24] All non-hydrogen atoms were refined anisotropically. The hydrogen atoms of water molecules in these complexes were located from the difference Fourier map and refined isotropically, the positions of other hydrogen atoms were generated geometrically (C-H bond fixed at 0.96 Å), assigned isotropic thermal parameters, and allowed to ride on their parent carbon atoms before the final cycle of refinement. Crystal data as well as details of data collection and refinement for complexes **1**-**6** are summarized in Table S1. The selected bond distances and bond angles are given in Table S2 in supporting information. Crystallographic data of 1-6 have been deposited in the Cambridge Crystallographic Data Centre as

supplementary publication with CCDC number: 1037113-1037118.

Note and Reference

1 E. Coronado and G. Minguez Espallargas, *Chem. Soc. Rev*., 2013, **42**, 1525; D. Zhao, D. J. Timmons, D. Yuan and H. C. Zhou, *Acc. Chem. Res.*, 2011, **44**, 123; S. Mukherjee and P. S. Mukherjee, *Acc. Chem. Res.*, 2013, **46**, 2556; D. Liu, J. P. Lang and B. F. Abrahams, *J. Am. Chem. Soc*., 2011, **133**, 11042.

2 J. R. Li, Q. Yu, Y. Tao, X. H. Bu, J. Ribas and S. R. Batten, *Chem.Commun.,* 2007, 2290; T. M. McDonald, W. R. Lee, J. A. Mason, B. M. Wiers, C. S. Hong and J. R. Long, *J. Am. Chem. Soc*., 2012, **134**, 7056; X. X. Li, H. Y. Xu, F. Z. Kong and R. H. Wang, *Angew Chem. Int. Ed*., 2013, **52**, 13769; X. X. Li, L. Cheng, W. H. Fang and G. Y. Yang, *Acta Chim. Sin.*, 2013, **71**, 179*;* F. L. Hu, S. L. Wang, J. P. Lang and B. F. Abrahams*, Sci. Reports.,* 2014, **4** 6815.

3 F. Jeremias, D. Fröhlich, C. Janiak and S. K. Henninger, *New J. Chem.*, 2014, **38**, 1846; H. X. Zhao, X. X. Li, J. Y. Wang, L. Y. Li and R. H. Wang, *ChemPlusChem*, 2013, **78**, 1491; X. J. Wang, P. Z. Li, Y. Chen, Q. Zhang, H. Zhang, X. X. Chan, R. Ganguly, Y. Li, J. Jiang and Y. Zhao, *Sci. Rep.*, 2013, **3**, 1149; U. Ravon, M. E. Domine, C. Gaudillère, A. Desmartin-Chomel and David Farrusseng, *New J. Chem.*, 2008, **32**, 937; D. Liu, Z. G. Ren, H. X Li, J. P. Lang, N. Y. Li and B. F. Abrahams, *Angew. Chem. Int. Ed.,* 2010, **49**, 4767.

4 Q. R. Fang, G. S. Zhu, Z. Jin, M. Xue, X. Wei, D. J. Wang and S. L. Qiu, *Cryst. Growth Des*., 2007, **7**, 1035; F. H. Cai, Y. Y. Ge, H. Y. Jia, S. S. Li, F. Sun, L. G. Zhang and Y. P. Cai, *CrystEngComm*, 2011, **13**, 67; Q. B. Bo, H. Y. Wang and D. Q. Wang, *New J. Chem.*, 2013, **37**, 380.

5 X. Z. Song, S. Y. Song, M. Zhu, Z. M. Hao, X. Meng, S. N. Zhao and H. J. Zhang, *Dalton Trans*., 2013, **42**, 13231; Q. Yan, Y. Lin, P. Wu, L. Zhao, L. Cao, L. Peng, C. Kong and L. Chen, *ChemPlusChem*, 2013, **78**, 86; L. F. Ma, L. Y. Wang, Y. Y. Wang, S. R. Batten and J. G. Wang, *Inorg. Chem.,* 2009, **48**, 915.

6 J. Gregory, Z. Q. McManus, Derek A.Wang, Beauchamp and Michael J. Zaworotko，*Chem. Commun.,* 2007, 5212; H. Furukawa, J. Kim, N. W. Ockwig, M. O'Keeffe and O. M. Yaghi. *J. Am. Chem. Soc.,* 2008, **130**, 11650; M. H. Zeng, H. H. Zou, S. Hu, Y. L. Zhou, M. Du and H. L. Sun, *Cryst. Growth Des.,* 2009, **9**, 4239; L. Liu, S. P. Huang, G. D. Yang, H. Zhang, X. L. Wang, Z. Y. Fu and J. C. Dai, *Cryst. Growth Des.*, 2010, **10**, 930.

7 G. Wu, X. F. Wang, T. Okamura, W. Y. Sun and N. Ueyama, *Inorg. Chem*., 2006, **45**, 8523; L. S. Long, *CrystEngComm*, 2010, **12**, 1354; Y. F. Han, X. Y. Li, L. Q. Li, C. L. Ma, Z. Shen, Y. Song and X. Z. You, *Inorg. Chem*., 2010, **49**, 10781; D. Sun, N. Zhang, R. B. Huang and L. S. Zheng, *Cryst. Growth Des*., 2010, **10**, 3699.

8 C. Li, D. S. Li, J. Zhao, Y. Q. Mou, K. Zou, S. Z. Xiao and M. Du, *CrystEngComm*, 2011, **13**, 6601; Z. M. Zhang, L. Y. Pan, W. Q. Lin, J. D. Leng, F. S. Guo, Y. C. Chen, J. L. Liu and M. L. Tong, *Chem. Commun*., 2013, **49**, 8081; G. Mukherjee and K. Biradha, *Cryst. Growth Des*., 2014, **14**, 419; L. Cui, G. P. Yang, W. P. Wu, H. H. Miao, Q. Z. Shi and Y. Y. Wang, *Dalton Trans*., 2014, **43**, 5823.

9 G. J. Xu, Y. H. Zhao, K. Z. Shao, Y. Q. Lan, X. L. Wang, Z. M. Su and L. K. Yan, *CrystEngComm*, 2009, **11**, 1842; B. Xu, Z. J. Lin, L. W. Han and R. Cao, *CrystEngComm*, 2011, **13**, 440; Y. L. Gai, F. L. Jiang, K. C. Xiong, L. Chen, D. Q. Yuan, L. J. Zhang, K. Zhou and M. C. Hong, *Cryst. Growth Des.,* 2012, **12**, 2079; S. Sengupta, S. Ganguly, A. Goswami, P. K. Sukul and R. Mondal, *CrystEngComm,* 2013, **15**, 8353.

10 T. W. Green and P. G. M. Wuts, *Protective Groups in Organic Synthesis*, Wiley-Interscience, New York, 1999, **736,** 518.

11 X. C. Cheng, X. H. Zhu and H. W. Kuai, *Z. Naturforsch*., 2013, **68b**, 1007.

12 M. H. Zeng, S. Hu, Q. Chen, G. Xie, Q. Shuai, S. L. Gao and L. Y. Tang. *Inorg. Chem.,* 2009, **48**, 7070; H. N. Wang, X. Meng, C. Qin, X. L. Wang, G. S. Yang and Z. M. Su. *Dalton Trans.,* 2012, **41**, 1047.F. L. Hu, W. Wu, P. Liang, Y. Q. Gu, L. G. Zhu, H. Wei and J. P. Lang, *Cryst. Growth Des.,* 2013, **13**, 5050; H. J. Cheng, H. X. Li, Z. G. Ren, C. N. Lü, J. Shi and J. P. Lang *CrystEngComm*., 2012,**14**, 6064; H. J. Cheng, B. Wu, L. W. Zhu, Ch. Y. Ni, M. Dai, H. X. Li, Z. G. Ren and J. P. Lang, *Inorg. Chem. Commun.,* 2013, **31**, 13.

13 Z. G. Li, G. H. Wang, H. Q. Jia, N. H. Hu, J. W. Xu and S. R. Batten, *CrystEngComm, 2008, **10**, 9*83; G. X. **L**iu, Y. Q. Huang, Q. Chu, T. Okamura, W. Y. Sun, H. Liang and N. Ueyama*, Cryst. Growth Des.,* 2008**, 8**, 3233; H. He, D. Collins, F. Dai, X. Zhao, G. Zhang, H. Ma *and D. Sun, Cryst. Growth D**es.,*** 2010, **10**, 895.

14 X. J. Li, X. L. Weng, R. J. Tang, Y. M. Lin, Z. L. Ke, W. B. Zhou and R. Cao, *Cryst. Growth Des*., 2010, **10**, 3228; X. J. Li, Y. Z. Cai, Z. L. Fang, L. J. Wu, B. Wei and S. Lin, *Cryst. Growth Des*., 2011, **11**, 4517; X. J. Li, X. F. Guo, X. H. Xu, G. C. Ma and S. Lin, *Inorg. Chem. Commun*., 2013, **27**, 105.

15 Y. Y. Xu, Y. Y. Xing, X. Y. Duan, Y. Z. Li, H. Z. Zhu and Q. J. Meng, *CrystEngComm*, 2010, **12**, 567; Y. Q.Yang, J. Yang, W. Q. Kan, Y. Yang, J. Guo and J. F. Ma, *Eur. J. Inorg. Chem.* 2013, 280; F. J. Liu, D. Sun, H. J. Hao, R. B. Huang and L. S. Zheng, *CrystEngComm*, 2012, **14**, 379; L. Dobrzanska, G. O. Lloyd and L. J. Barbour, *New J. Chem.* 2007, **31**, 699.

16 H. W. Kuai, X. C. Cheng, L. D. Feng and X. H. Zhu, *Z. Anorg. Allg. Chem*., 2011, **637**, 1560.

17 G. X. Liu, K. Zhu, H. Chen, R. Y. Huang and X. M. Ren, *CrystEngComm*, 2008, **10**, 1527. F. L. Hu, Y. Mi, Y. Q. Gu, L. G. Zhu, S. L. Yang, H. Wei and J. P. Lang, *CrystEngComm.,* 2013, **15**, 9553; C. N. Lü, M. M. Chen, W. H. Zhang, D. X. Li, M. D. and J. P. Lang, *CrystEngComm.,* 2015, **17**, 1935.

18 M. H. Zeng, S. Hu, Q. Chen, G. Xie, Q. Shuai, S. L. Gao and L.Y. Tang, *Inorg. Chem.,* 2009, **48**, 7070; P. Kanoo, G. Mostafa, R. Matsuda, S. Kitagawa and T. K. Maji, *Chem. Commun*., 2011, **47**, 8106.

19 R. A. Agarwal, A. Aijaz, C. Sañudo, Q. Xu and P. K. Bharadwaj, *Cryst. Growth Des.*, 2013, **13**, 1238; C. B. Tian, H. B. Zhang, Y. Peng, Y. E. Xie, P. Lin, Z. H. Li and S. W. Du, *Eur. J. Inorg. Chem.,* 2012, 4029.

20 D. Sarma, K. V. Ramanujachary, S. E. Lofland, T. Magdaleno and S. Natarajan, *Inorg. Chem*., 2009, **48**, 11660; X. Y. Dong, B. Li, B. B. Ma, S. J. Li, M. M. Dong, Y. Y. Zhu, S. Q. Zang, Y. Song, H. W. Hou and T. C. W. Mak, *J. Am. Chem. Soc*., 2013, **135**, 10214.

21 M. C. Das and P. K. Bharadwaj, *J. Am. Chem. Soc*., 2009, **131**, 10942.

22 B. F. Hoskins , R. Robson and D. A. Slizys, *J. Am. Chem. Soc*., 1997, **119**, 2952.

23 G. M. Sheldrick, SHELXS97, Program for Crystal Structure Solution; University of Göttingen: Göttingen, Germany, **1997**; G. M. Sheldrick, SHELXL97, Program for Crystal Structure Refinement; University of Göttingen: Göttingen, Germany, **1997**.